Photonic quantum entanglement

A I Smith, C M Steenkamp and M S Tame

Department of Physics, SU, Matieland 7602, RSA

E-mail: andre12smith@gmail.com

Abstract.

Path entanglement is an essential tool in quantum information and quantum communication protocols. We study the generation and measurement of path entangled photon states using pairs of single photons generated by spontaneous parametric down-conversion (SPDC). Path entanglement is generated using a Mach-Zender (MZ) interferometer in one arm of the SPDC setup. We characterise the MZ interferometer as well as perform standard tests to indicate whether entanglement is present, including protocols on determining the quality of the photons generated. These tests include a second-order correlation measurement and a visibility measurement. These two tests determine the quality of the single photons being generated and the quality of interference of a photon with itself, respectively.

1. Introduction

Entanglement is a valuable resource in the development of quantum computers and quantum information systems [1]. It has two common definitions: the first states that a composite system which forms some state is entangled if it is not separable [2]. The second states that entangled states are states that cannot be simulated by classical correlations [3].

In terms of the example given in Fig. 1 the first definition would say the system is entangled if the state of photon 1 could not be separated from the state of photon 2. This is the case in this example as when one of the photons is measured as $|H\rangle$ the other must be measured as $|V\rangle$ and vice versa, where $|H\rangle$ and $|V\rangle$ correspond to a horizontal and vertical polarised photon, respectively. This means that the measured outcomes are necessarily dependant on each other.

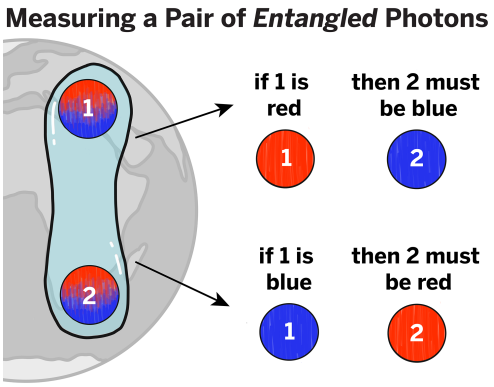

Figure 1. Example image of two photons generated in the state $|\Psi\rangle = \frac{1}{\sqrt{2}}(|H\rangle|V\rangle + |V\rangle|H\rangle)$ being measured. Here $|H\rangle$ is shown as red and $|V\rangle$ is shown as blue.

For the second definition the example given in Fig. 1 would be considered entangled if the measured outcome of the system could not be simulated by a classical system. A classical equivalent for this system would be a system where randomly one photon is produced in the state $|H\rangle$ and based on this the other is in the state $|V\rangle$.

Any set of measurements on this classical state will show only classical correlations, whereas for the state $|\Psi\rangle$ in Fig. 1, there are measurements outcomes that cannot be simulated classically [3].

The scenario shown in Fig. 1 is an example of polarisation entanglement. For this research, single-photon entanglement, also know as path entanglement is used.

Path entanglement is a form of entanglement which instead of making use of two photons that can be measured in $|H\rangle$ or $|V\rangle$, makes use of two paths. Each path can be measured in the states $|1\rangle$ and $|0\rangle$, where $|1\rangle$ denotes a photon detection and $|0\rangle$ denotes no photon detection or a vacuum detection. An example setup for producing this entanglement can be seen in Fig. 2.

The state created in the example in Fig. 2 is $|\Psi\rangle = \frac{1}{\sqrt{2}}(|1\rangle_1 |0\rangle_2 + |0\rangle_1 |1\rangle_2)$, where the subscripts denote the path the detection is made in. This system is known to be an entangled system [4, 6]. In this case the polarisation of the photon is not indicated as the photon has the same polarisation in each path.

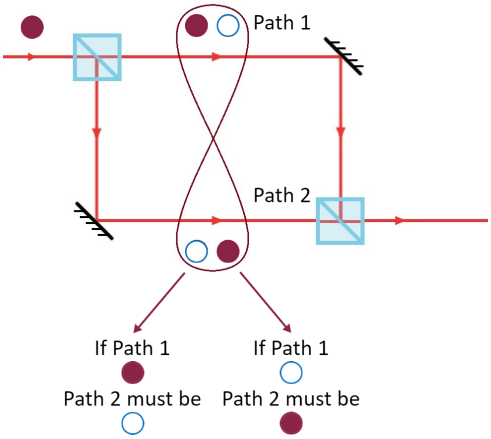

Figure 2. Example setup for producing path entanglement inside a Mach-Zehnder interferometer.

2. Setup

To generate single-photon path entanglement the setup in Fig. 3 was built. In the figure the single-photon source is a BBO crystal. Detector A is used as a heralding detector to infer the existence of a photon which can be measured by either detector B or C. A Mach-Zehnder (MZ) interferometer is placed in the heralded arm, this consists of two 50/50 beamsplitters as well as two mirrors, one of which is placed on a translation stage, and set such that the two paths interfere coherently.

In the image a line can be seen drawn through the MZ interferometer, this is used to distinguish the generation and analysis part of the interferometer. This line can also be used to represent where entanglement is present.

It should also be noted that there are three neutral density (ND) filters present. These filters are added as the beamsplitters used are not exactly 50/50, thus the ND filters are added to compensate for the beamsplitters. The ND filter labelled $ND1$ is used to compensate for BS 1 which has a higher transmission than reflectance in the generation half of the MZ interferometer. The filter ND 2 is used to compensate for BS 2, which also has a higher transmission than reflectance, in the analysis half of the MZ interferometer. The final filter ND 3 is used to compensate for the polarising beamsplitter, which is used when probing the state.

The half-wave plates (HWP) are used to probe the generated path entangled state together with the polarising beamsplitter, and initially all have their fast axes set to zero

3. Method

To generate single-photon path entanglement, the ND filters are set such that the outputs of each of the beamsplitters are equal. Single photons are sent through the setup and the mirror mounted on the translation stage is then set such that the two arms of the MZ interferometer interfere coherently.

To probe the state of the generated path entanglement we follow Ref [4]. The two paths within the MZ interferometer are set to be distinguishable. This is done using two HWP's

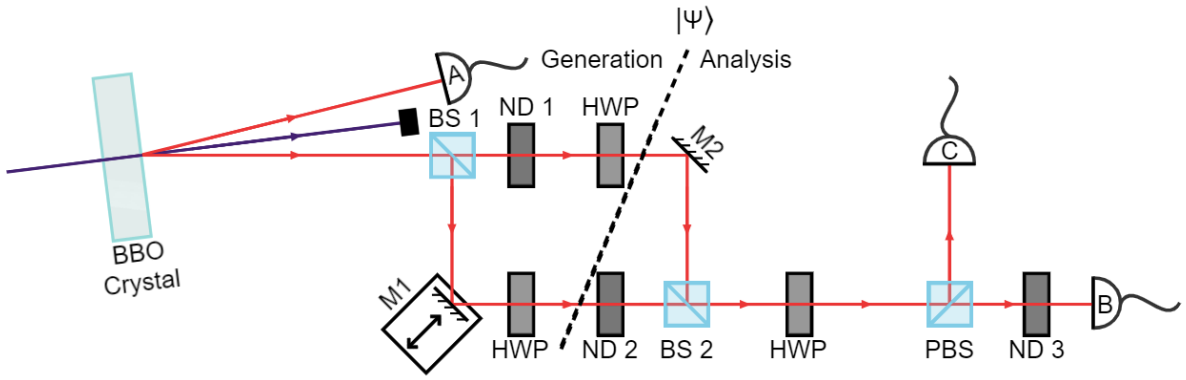

Figure 3. A simplified diagram of the setup used to generate single-photon entanglement.

Table 1. Theoretical prediction of what is expected when sending the $|\Psi'\rangle = |+\rangle$ state through a HWP at angle θ.

θ	$\|H\rangle$ mapping	$\|V\rangle$	$\|\Psi''\rangle$
0°	$\|H\rangle$	$-\|V\rangle$	$\|-\rangle$
22.5°	$\|+\rangle$	$\|-\rangle$	$\|H\rangle$
45°	$\|V\rangle$	$\|H\rangle$	$\|+\rangle$
67.5°	$-\|-\rangle$	$\|+\rangle$	$\|V\rangle$
90°	$-\|H\rangle$	$\|V\rangle$	$\|-\rangle$

within the interferometer, one of which, the lower path, has fast axis its set to a 45° angle. This results in the two arms within the MZ interferometer having orthogonal polarisations and $|\Psi\rangle = \frac{1}{\sqrt{2}}(|H\rangle_1 |0\rangle_2 + |0\rangle_1 |V\rangle_2)$. When recombining the two paths at the analysis stage the output state after BS 2 is given by

$$\left|\Psi'\right\rangle = \frac{1}{\sqrt{2}}\left(|H\rangle + \mathrm{e}^{i\phi}|V\rangle\right), \tag{1}$$

where ϕ is the phase gained inside the MZ, however since the paths were set such that they interfer coherently, $\phi = 0$. This results in equal detections in detectors B and C. Since equal frequency of detection is present, equal probability can be inferred for detection. The HWP located outside of the MZ interferometer is then used to interfere the output of the two paths to analyse the state further by rotating the angle of the HWP. This produces the final state

$$\left|\Psi''\right\rangle = \frac{1}{\sqrt{2}}\Big(\big(\cos 2\theta\,|H\rangle + \sin 2\theta\,|V\rangle\big) + \big(\sin 2\theta\,|H\rangle - \cos 2\theta\,|V\rangle\big)\Big), \tag{2}$$

where θ is the change of the fast axis of the HWP.

4. Results and Discussion

To ensure that all experiments are done using single photons a second-order correlation ($g^{(2)}$) test is performed. This test found $g^{(2)} = 0.0043 \pm 0.0019$ which is well within the bound $g^{(2)} \leq 0.5$ to ensure single photons are being produced [5].

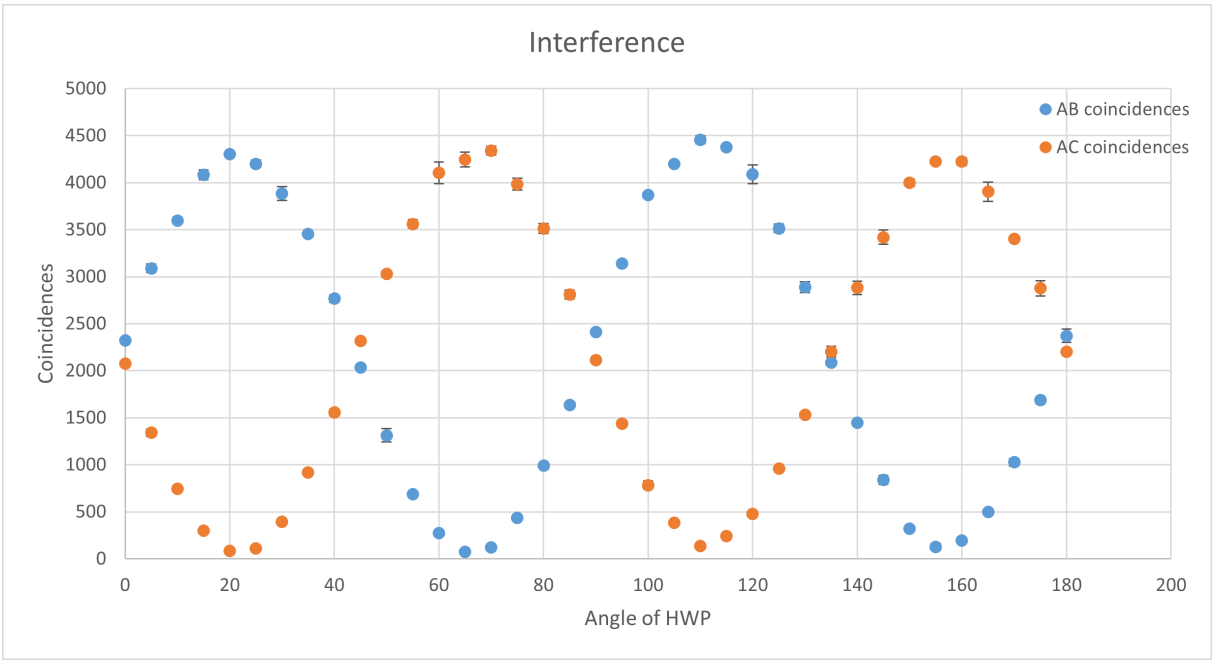

Figure 4. Interference data captured by increasing angle θ by 5° increments over a $5s$ interval. Error bars represent the standard deviation of data at each angle.

When interfering the output of the two paths it is expected that the output state $|\Psi''\rangle$ will behave as shown in Table 1. In Table 1 the output state fluctuates from equal detections in B and C to full detections in one, back to equal detections and then full detections in the other.

Comparing the prediction in Table 1 to the data obtained in Fig. 4, the same oscillation can be seen where the number of detected photons alternates between $|H\rangle$ polarisation to $|V\rangle$ polarisation, as seen by the change in number of detections in detectors B and C (coincidences with A within $8ns$), which represent the detection of $|H\rangle$ and $|V\rangle$ polarisation photons.

To test the presence and the quality of entanglement in the system the concurrence (C_N) is determined. This is done by using

$$C_N = V - \sqrt{y_c}, \tag{3}$$

for post-selected entanglement. In Eq. 3, V represents the visibility, which is a measure of the quality of the interference observed in Fig. 4, and y_c is a measure of the degree of contamination due to higher order interactions [4]. The visibility (V) is determined by using

$$V = |P_{01} - P_{10}|, \tag{4}$$

where P_{10} and P_{01} are the normalised probabilities of a photon detection in path 1 or 2, respectively [4]. Determining y_c is done by using

$$y_c = 2\left(\frac{N}{N-1}\right)\frac{p_0 p_2}{p_1^2}, \tag{5}$$

where N is the number of modes present in the system, in this case 2, and p_0, p_1 and p_2 represent the probability of no photons, one photon and two photons being present in the MZ interferometer [4].

When using the data in Fig. 4 along with the given equations it is found that $V = 0.9647 \pm 0.5684 \times 10^{-3}$, which implies high quality interference and $y_c = 0.001284 \pm 0.003032$.

For entanglement to be present it is required that $y_c \leq V^2$ [4]. The experimental value obtained for y_c is several orders of magnitude smaller than the required boundary for entanglement to be present. This implies the existence of entanglement in the system with low higher-order contamination. Finally it is found that $C_N = 0.9499 \pm 0.03325$, this implies the existence of high quality entanglement which could be used in quantum information protocols.

5. Conclusion

The results obtained imply the generation of high quality path entanglement, meaning the setup was successful in its aim to generate path entanglement, which can be applied in quantum communication, quantum sensing and quantum imaging applications.

References

[1] Nielsen M A, Chuang I L 2010 *Quantum computation and quantum information* (Cambridge: Cambridge press).
[2] Horodecki R, Horodecki P, Horodecki M and Horodecki K 2009 *Rev. Mod. Phys.* **81**, 865–942.
[3] Masanes L, Liang Y and Doherty A C 2008 *Phys. Rev. Lett.* **100** 090403.
[4] Papp S B, Choi K S, Deng H, Lougovski P, van Enk S J and Kimble H J 2009 *Science* **324**, 764–68.
[5] Loudon R 2000 *The Quantum Theory of Light* (Oxford: Oxford University Press).
[6] van Enk S J 2006 *Phys. Rev. A* **74** 026302.